



**AAS 06-072**

# ENTRY, DESCENT, AND LANDING CHALLENGES OF HUMAN MARS EXPLORATION

Wells, G., Lafleur, J., Verges, A., Manyapu, K.,  
Christian, J., Lewis, C., Braun, R.

Georgia Institute of Technology

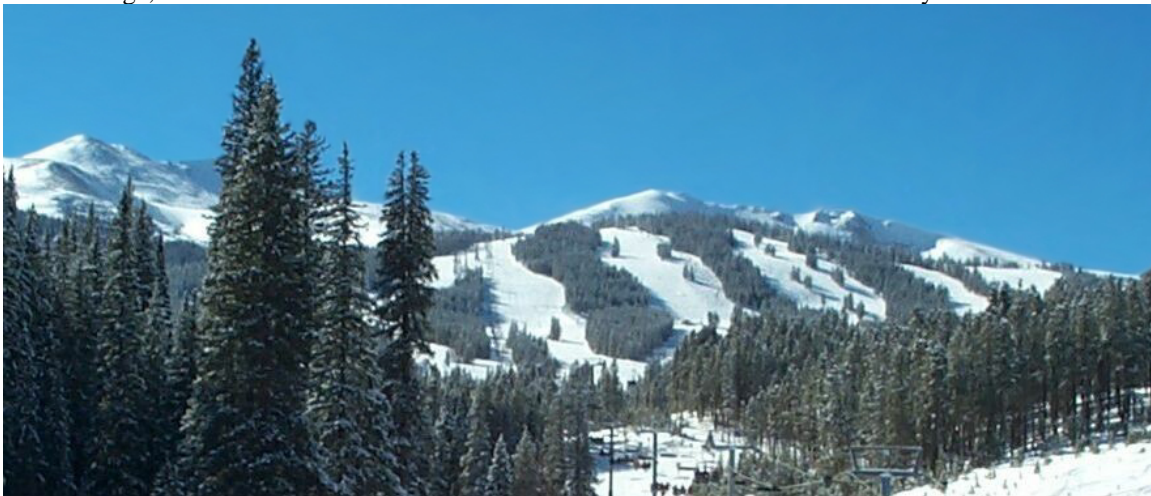
---

## **29th ANNUAL AAS GUIDANCE AND CONTROL CONFERENCE**

---

February 4-8, 2006  
Breckenridge, Colorado

Sponsored by  
Rocky Mountain Section



AAS Publications Office, P.O. Box 28130 - San Diego, California 92198

## ENTRY, DESCENT, AND LANDING CHALLENGES OF HUMAN MARS EXPLORATION

**Wells, G.<sup>\*</sup>, Lafleur, J.<sup>†</sup>, Verges, A.<sup>‡</sup>, Manyapu, K.<sup>§</sup>,  
Christian, J.<sup>\*\*</sup>, Lewis, C.<sup>††</sup>, Braun, R.<sup>‡‡</sup>,**

Near-term capabilities for robotic spacecraft include a target of landing 1 - 2 metric ton payloads with a precision of about 10 kilometers, at moderate altitude landing sites (as high as +2 km MOLA). While challenging, these capabilities are modest in comparison to the requirements for landing human crews on Mars. Human Mars exploration studies imply the capability to safely land 40 - 80 metric ton payloads with a precision of tens of meters, possibly at even higher altitudes. New entry, descent and landing challenges imposed by the large mass requirements of human Mars exploration include: (1) the potential need for aerocapture prior to entry, descent and landing and associated thermal protection strategies, (2) large aeroshell diameter requirements, (3) severe mass fraction restrictions, (4) rapid transition from the hypersonic entry mode to a descent and landing configuration, (5) the need for supersonic propulsion initiation, and (6) increased system reliability. This investigation explores the potential of extending robotic entry, descent and landing architectures to human missions and highlights the challenges of landing large payloads on the surface of Mars.

---

<sup>\*</sup> Graduate Research Assistant. Mr. Wells is affiliated with the Georgia Institute of Technology, School of Aerospace Engineering, 270 Ferst Drive, Atlanta, GA 30332.

E-mail: grant\_wells@ae.gatech.edu. Phone: (404) 894-7783, Fax: (404) 894-2760.

<sup>†</sup> Undergraduate Research Assistant. Mr. Lafleur is affiliated with the Georgia Institute of Technology, School of Aerospace Engineering, 270 Ferst Drive, Atlanta, GA 30332.

E-mail: jarret.m.lafleur@gatech.edu. Phone: (404) 894-7783, Fax: (404) 894-2760.

<sup>‡</sup> Undergraduate Research Assistant. Ms. Verges is affiliated with the Georgia Institute of Technology, School of Aerospace Engineering, 270 Ferst Drive, Atlanta, GA 30332. E-mail: averges@gatech.edu. Phone: (404) 894-7783, Fax: (404) 894-2760.

<sup>§</sup> Undergraduate Research Assistant. Ms. Manyapu is affiliated with the Georgia Institute of Technology, School of Aerospace Engineering, 270 Ferst Drive, Atlanta, GA 30332. E-mail: kavyakamal@gatech.edu. Phone: (404) 894-7783, Fax: (404) 894-2760.

<sup>\*\*</sup> Graduate Teaching Assistant. Mr. Christian is affiliated with the Georgia Institute of Technology, School of Aerospace Engineering, 270 Ferst Drive, Atlanta, GA 30332.

E-mail: john.a.christian@gatech.edu. Phone: (404) 894-7783, Fax: (404) 894-2760.

<sup>††</sup> Undergraduate Research Assistant. Ms. Lewis is affiliated with the Georgia Institute of Technology, School of Aerospace Engineering, 270 Ferst Drive, Atlanta, GA 30332. E-mail: charity@gatech.edu.

Phone: (404) 894-7783, Fax: (404) 894-2760.

<sup>‡‡</sup> Associate Professor. Dr. Braun is affiliated with the Georgia Institute of Technology, School of Aerospace Engineering, 270 Ferst Drive, Atlanta, GA 30332. E-mail: robert.braun@ae.gatech.edu. Phone: (404) 385-6171, Fax: (404) 894-2760.

## **INTRODUCTION**

The United States has successfully landed five robotic systems on the surface of Mars. These systems all had a landed mass below 0.6 metric tons (t), had landed footprints on the order of hundreds of kilometers and landing sites below -1 km MOLA elevation due the need to perform entry, descent and landing (EDL) operations in an environment with sufficient atmospheric density. Current plans for human exploration of Mars call for the landing of 40 - 80 t surface elements at scientifically interesting locations within close proximity (10's of meters) of pre-positioned robotic assets. As shown in this investigation, these constraints require the space qualification of new EDL approaches and technologies.

In this investigation, the challenges associated with the successful entry, descent and landing of large mass payloads for human exploration systems (20 t to 100 t) using an entry, descent and landing architecture extended from current robotic exploration technology is illustrated. The mission approach investigated begins with an aerocapture maneuver into Martian orbit. After achieving orbit, the spacecraft enters the Martian atmosphere to land on the surface. Two terminal descent options are considered: (1) propulsively and (2) parachute deceleration followed by a propulsive descent segment to the surface. Payload mass limits delivered to the surface of Mars are shown for spacecraft which use a single heatshield for aerocapture and entry-from-orbit (termed a dual-use heatshield) and for spacecraft which use separate heatshields for aerocapture and entry-from-orbit (termed single-use heatshields).

## **DISCUSSION**

### **Atmosphere**

The atmospheric density on Mars varies significantly with time-of-year, time-of-day, dust-level (atmospheric opacity) and latitude. To account for the effects of each of these variables, a design atmospheric density profile was constructed from approximately one-thousand runs of Mars-GRAM 2005 in which month, time of day, dust level, and latitude for the years of 2030 and 2031 were randomly varied.

Cumulative distribution functions of density were constructed for each altitude from -8 km to 152 km MOLA. The density at the 30% point on each cumulative distribution function was chosen. The resulting atmosphere was chosen for this investigation and is shown in Figure 1. The resulting density profile gives a 0 km density of  $0.0124 \text{ kg/m}^3$ . Approximately 70% of the atmospheric density profiles simulated had a higher 0 km density.

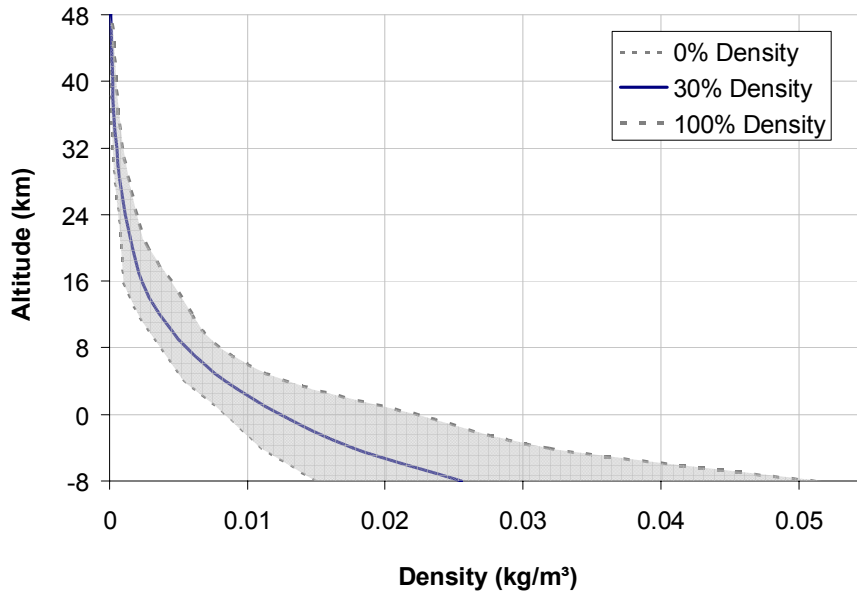


**Figure 1 Design Martian atmospheric density profile representing the 70%-pessimistic (30% cumulative distribution function) case for over 1000 runs of Mars-GRAM 2005. The shaded region shows the entire span of the Mars-GRAM runs.**

### **Aeroshell Shape and Size**

The aeroshell used in this analysis is an Apollo capsule shape, photographically scaled to 10 m and 15 m diameter. A scaled Apollo capsule was chosen because capsules and other blunt body designs compare favorably to slender-body designs that offer more lift and higher L/D at the expense of drag (and therefore final altitude).<sup>1</sup> Entry system lift-to-drag ratios of 0.3 and 0.5 were considered.

From a vehicle packaging standpoint, a large blunt body design is flexible. The 15 m diameter can accommodate high-volume components such as a surface habitat or descent stage. The capsule shape also allows a large portion of the mass to be packaged near the front of the vehicle for improved aerodynamic stability. The blunt body design does not require significant vehicle reorientation during the EDL profile for system deployments (e.g., parachute deployment, heatshield separation, propulsive initiation). In addition, in all flight regimes, acceleration is imparted to the vehicle in the same direction, thus facilitating the design of crew positions with respect to g-tolerance.

The EDL systems considered in this investigation assume development of a heavy lift launch vehicle capable of lofting a 10 - 15 m diameter payload in one piece. Ultimately, this challenge must be weighed against the difficulty of launching a human-rated aeroshell in several pieces and then assembling and certifying it in LEO, or limiting the Mars exploration architecture to much smaller diameters and entry masses (with possible surface assembly).

## RESULTS

### Aerocapture

Direct entry from a heliocentric arrival trajectory can have a significant mass advantage and operations simplicity. However, direct entry does not offer the mission design flexibility to accommodate uncertainties in the Martian atmosphere such as dust storms. Orbit insertion before entry will reduce the peak deceleration on human crews, and fits well with potential orbit rendezvous requirements for Earth return. For these reasons, this investigation assumes a human exploration architecture in which orbit insertion precedes landing. Orbit insertion around a planet with an atmosphere may be done with propulsion, aerobraking, or by aerocapture.

Propulsive orbital insertion is the lowest risk approach, but is mass prohibitive, as shown in Figure 2. Arrival velocity at Mars has large impact on propellant mass fraction, and a mass fraction greater than 0.3 is required. For short duration interplanetary transfers with associated high entry velocities, a mass fraction in the range of 0.7-0.8 may be required, prohibiting this architecture selection. The choice of parking orbit has a moderate impact on the propellant mass fraction required, while the choice of fuel, liquid hydrogen (LH2) or methane (CH4), has a negligible impact on propellant mass fraction. The length of time required for aerobraking makes its use for orbit insertion around Mars unlikely for human missions. To reduce initial mass requirements, aerocapture is likely to be required for human Mars exploration and is assumed in this investigation. Since aerocapture has not been flight proven, aerocapture technology is deemed a likely candidate for validation by precursor robotic missions.

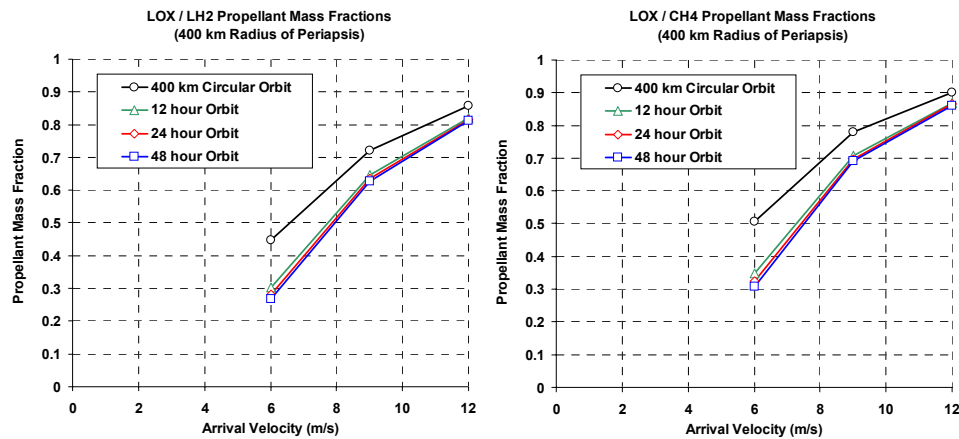


**Figure 2 Mass fraction estimates for propulsive orbital insertion at Mars.**

Aerocapture slows a spacecraft from hyperbolic to orbital speed in a single pass through the atmosphere of a planet. A schematic of aerocapture is depicted in Figure 3 for an orbiter mission. During aerocapture, a spacecraft first enters the atmosphere of a planet from an inbound hyperbolic orbit. This pass through the atmosphere slows the spacecraft, and when the spacecraft exits the atmosphere, it has an orbital energy equal to that of the desired orbit around the planet. After decelerating in the atmosphere, the

heatshield may be jettisoned. When apoapsis of the desired orbit is reached, a propulsive maneuver is performed to raise the periapsis of the spacecraft's orbit. At periapsis, another propulsive maneuver may be performed to correct for error in the orbit.

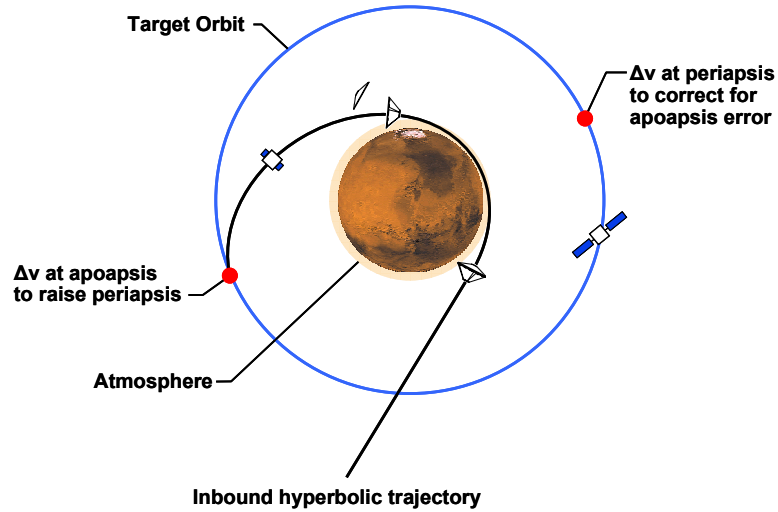


**Figure 3 Aerocapture into orbit around Mars.**

Aerocapture trajectories are generally constrained by the following limits, depicted in Figure 4.

1. The trajectory with the most shallow flight path angle that meets the exit energy constraint (lift-down). This trajectory has the lowest peak heating rate and lowest peak deceleration, but the highest integrated heat load.
2. The trajectory with the steepest flight path angle that meets the exit energy constraint (lift-up). This trajectory has the highest peak heating rate and the highest peak deceleration, but the lowest integrated heat load.
3. The flight path angle that achieves the specified peak deceleration limit with a lift-up entry (5 g). The vehicle flies lift-up until peak deceleration, and after the limit is reached, uses bank angle control to achieve the desired exit energy. The 5 g limit was assumed to be the maximum tolerable deceleration for short periods by a crew of de-conditioned astronauts.

A study of aerocapture trajectories was performed to determine bounding entry velocities that would allow for at least a  $1^\circ$  aerocapture entry corridor width into a 400 km circular orbit around Mars. This was done to accommodate a conservative, assumed navigation requirement of  $\pm 0.5^\circ$  on flight path angle at arrival. As shown in Figure 4, for a vehicle  $L/D = 0.3$ , this corridor width limit yields an entry velocity constraint between 6 and 8.8 km/s. This entry velocity range corresponds to a wide range of interplanetary trajectory options.<sup>2</sup> Therefore, with current navigation assumptions, an  $L/D$  of 0.3 is sufficient for Mars aerocapture.

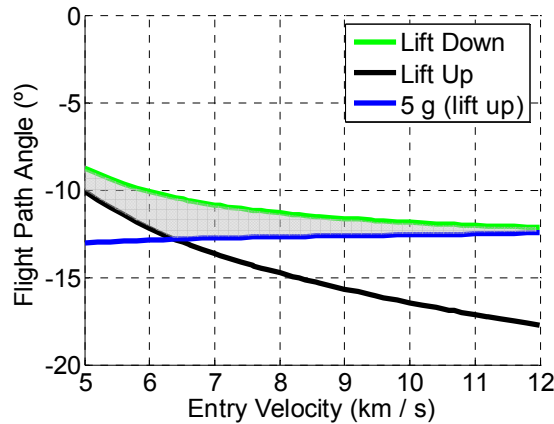


**Figure 4 An aerocapture corridor showing each boundary and the physical corridor (shaded) for  $L/D = 0.3$ .**

### Entry from Orbit

After aerocapture, a vehicle delivering humans or cargo to the surface must perform entry, descent and landing. For the purposes of this study, an entry velocity of 4 km/s was assumed in order to determine the entry corridor based on: (a) the lift-down trajectory with the most shallow flight path angle that allows for entry without skipping out (the overshoot trajectory) and (b) the lift-up trajectory with the steepest flight path angle having a peak deceleration of 5 g (the undershoot trajectory). The 5 Earth-g limit again being considered the maximum deceleration that de-conditioned astronauts can tolerate for short durations. The range of trajectories between the lift-down and lift-up flight paths is the entry corridor. Figure 5 shows the final altitudes of the trajectories as a function of mass with varying end conditions of Mach 2, 3 and 4 for both the lift-up and lift-down trajectories. These curves provide insight as to how much altitude is available to provide descent deceleration via parachutes or propulsion or some combination.

The heatshield sizing study results in the two sets of data shown in Figure 5: (a) a dual-use heatshield set, from which there is essentially no mass change before the entry from orbit and (b) a single-use heatshield set, from which a significant mass change occurs due jettisoning the outer aerocapture heatshield before entry from orbit. Data are shown for an  $L/D$  of 0.3 and 0.5, a 10- and 15-m aeroshell diameter, and masses ranging from 20 to 100 t.

From Figure 5, it is apparent that the aeroshell diameter (ballistic coefficient) has a large effect in slowing the vehicle resulting in higher altitudes for a given Mach number. These figures also highlight the difficulty of slowing a human-scale vehicle with high ballistic coefficient (high entry mass and/or small diameter) before impact due to the low-density Mars atmosphere. The heavy dependence on ballistic coefficient tends to favor larger aeroshells. Since some cases do not reach Mach 2 before 0 km altitude, parachutes or more novel aerodynamic decelerators deployed at Mach 3 may be required for human-scale entry systems (depending on the altitude of the desired landing site). Much of the Martian surface between latitudes  $60^{\circ}S$  and  $60^{\circ}N$  has an elevation in the shaded regions of Figure 5.

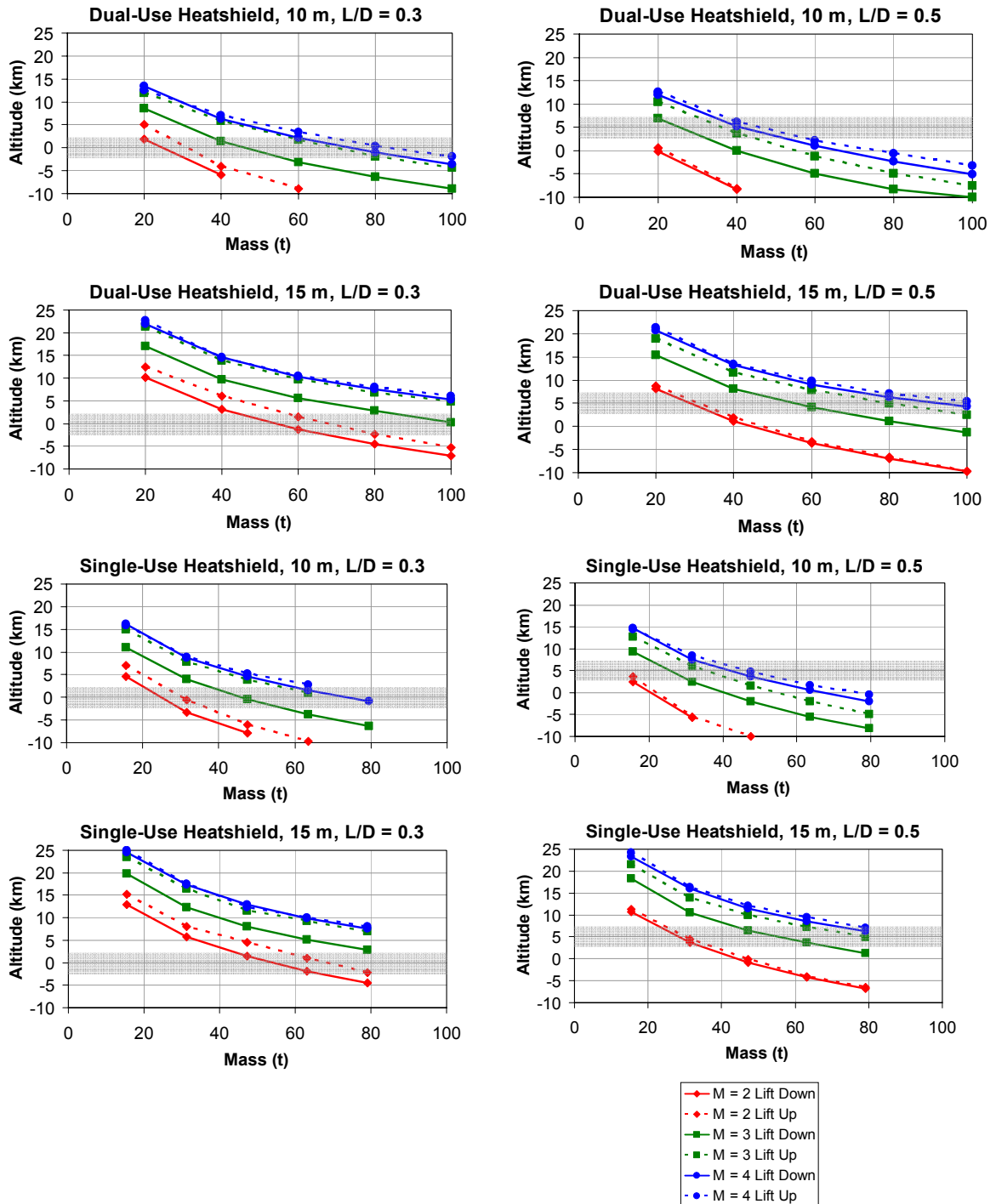


**Figure 5** Mach 2, 3 and 4 transition altitudes as a function of entry mass for 10 m and 15 m aeroshells with L/Ds of 0.3 and 0.5 considering both single-use and dual-use heatshields.

Note that the Mach number transition altitudes shown in Figure 5 are given for the entire corridor available to the vehicle and do not account for any navigational constraints.

## Propulsive Descent

A gravity turn is a propulsive descent maneuver in which a spacecraft's thrust vector is maintained in an orientation opposite its velocity vector. This gravity turn control law was originally developed for the Lunar Surveyor landings. Typically, the termination of a gravity turn will be when nadir angle, relative velocity, and height above ground level are all zero. In this study, two-dimensional gravity turn trajectories were assumed to occur over a flat Mars. The free body diagram shown in Figure 6 and associated equations of motion given in Eq. (1) were used. Here,  $mg$  is the gravitational force on the vehicle,  $T$  is thrust provided by the vehicle's propulsion system,  $D$  is aerodynamic drag,  $L$  is aerodynamic lift,  $v$  is the vehicle's velocity, and  $\psi$  is the nadir angle.

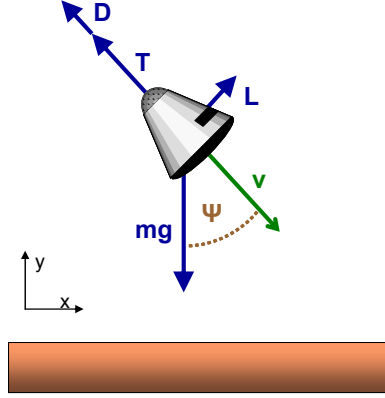


**Figure 6** Free body diagram showing the conventions and notation used for gravity turns.

$$\begin{aligned}\sum F_y &= ma_y = T \cos \psi - mg + D \cos \psi + L \sin \psi \\ \sum F_x &= ma_x = -T \sin \psi - D \sin \psi + L \cos \psi\end{aligned}\quad (1)$$

Eq. (1) above can be manipulated to yield the two nonlinear differential equations shown in Eq. (2). In these equations,  $a_L$  is instantaneous acceleration due to lift (i.e. lift force divided by vehicle mass),  $a_T$  is instantaneous acceleration due to thrust, and  $a_D$  is instantaneous acceleration due to drag.

$$\begin{aligned}\dot{\psi} &= \frac{a_L - g \sin \psi}{v} \\ \dot{v} &= g \cos \psi - a_T - a_D\end{aligned}\quad (2)$$

In this investigation, Eqs. (1) and (2) were integrated to yield trajectory data over time and to ultimately generate thrust and  $\Delta V$  requirements using a Matlab code. Three assumptions were made in the calculation of the propulsive descent trajectory: lift is zero, thrust is constant, drag varies with Mach number according to a profile scaled to the vehicle's supersonic drag coefficient.

It was also desired that a contingency hover and crossrange capability of 500 m be built into the powered descent profile for obstacle avoidance. This maneuver consists of

three parts: crossrange acceleration, crossrange deceleration, and a vertical descent as shown in Figure 7.

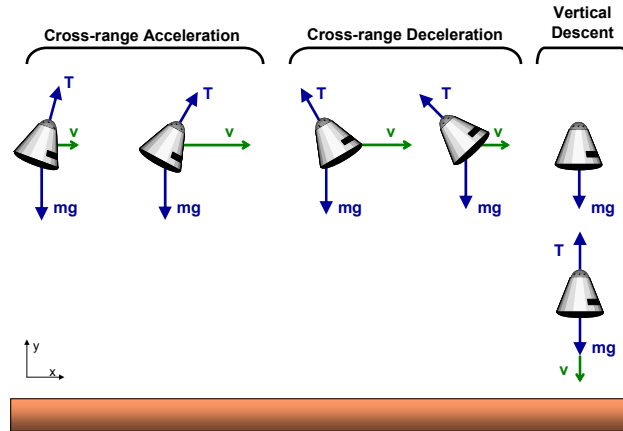


**Figure 7 Schematic of the crossrange maneuver during propulsive descent.**

Propulsive descent was analyzed with and without Mach 3 deployment of a 30 m parachute. For the parachute cases, this system was jettisoned after its deceleration no longer exceeded that provided by the propulsion system.

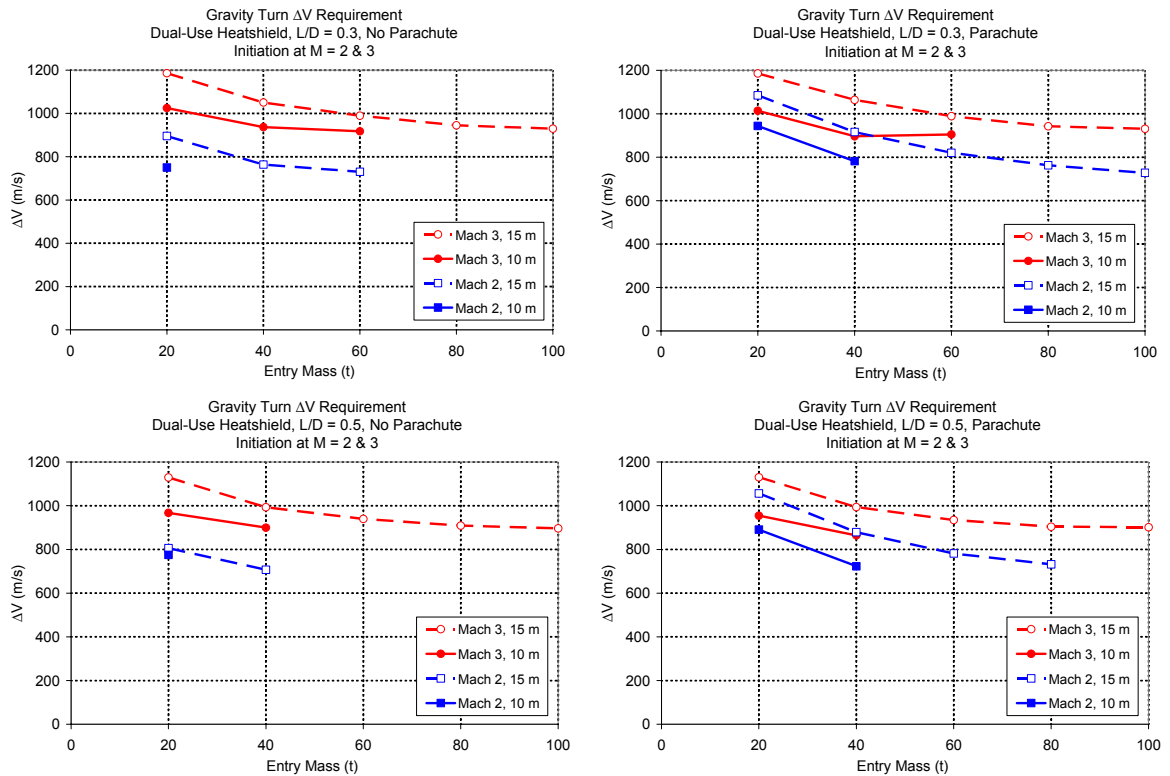


**Figure 8 Propulsive descent  $\Delta v$  requirements with and without a parachute for L/Ds of 0.3 and 0.5.**

Figure 8 shows that  $\Delta V$  requirement for a Mach 3 burn initiation does not change significantly with use of a parachute. This occurs because the parachute (deployed at Mach 3) is jettisoned after only a few seconds when the burn begins at Mach 3. When the gravity turn is initiated at Mach 2 for this same Mach 3 parachute deployment, the addition of the parachute raises overall  $\Delta V$  requirements due to higher gravity losses (because of the longer time spent at large flight path angles). However, it also substantially increases the range of masses which can be landed. This indicates that technology development of a Mach 3 deployable parachute could have substantial benefits for human missions to Mars.

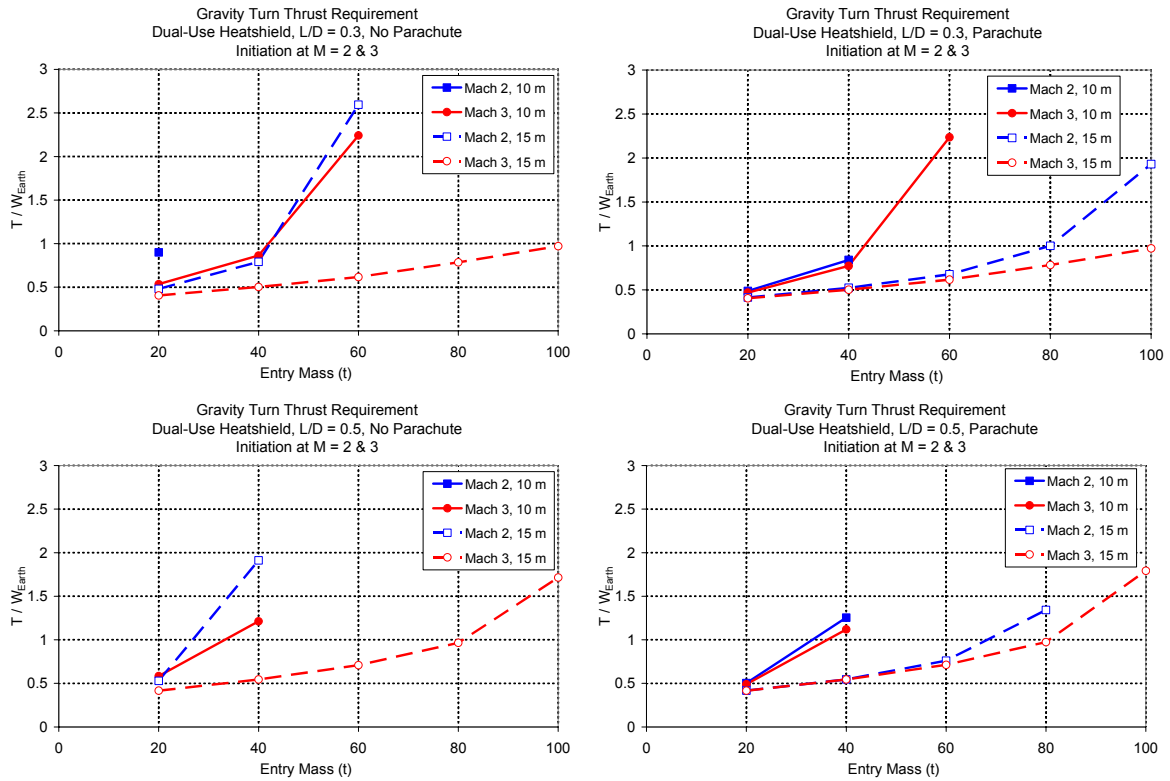


**Figure 9 Propulsive descent thrust requirements with and without a parachute for L/Ds of 0.3 and 0.5.**

Figure 9 shows that the thrust requirement also does not vary significantly between parachute and no-parachute cases with a burn initiation Mach number of 3. Again, however, when the gravity turn is initiated at Mach 2, the parachute substantially impacts the results. The thrust requirement is significantly lowered and the range of masses that can land is substantially increased.

### Weights and Sizing

As discussed above, previous human Mars exploration studies provide estimates of vehicle mass at aerocapture ranging from 20 t to 100 t. The weights and sizing analysis performed below is aimed at determining what fraction of this total mass is required by the EDL system to safely land on the Martian surface and how much mass remains for payload.

The mass of the entire EDL system was computed by combining the estimated masses of each of the major EDL subsystems. First-order sizing algorithms were used to estimate the mass of the heatshield,<sup>7</sup> main propulsion system, and reaction control system (RCS). Backshell and parachute masses were estimated as percentages of the vehicle mass at entry. Additionally, an EDL mass margin of 30% was included in all calculations. Details of the techniques used to size each of these subsystems are provided in the subsequent sections.

*Parachute.* The mass of the parachute system was estimated as a percentage of the total entry mass. Research indicated that parachute mass fractions vary widely, ranging anywhere from about 1% to as high as 8%. Parachute mass was traded within this range to determine what percentages generate a system that matches or exceeds the performance of the propulsive-only options (i.e. cases that do not use parachutes to decelerate). Details of this trade may be found below in the *Overview of Sizing Results* section (see Figure 11).

*Backshell.* As with the parachute system, the backshell mass was calculated using a historical mass percentage. This device was estimated as 15% of the entry mass. Note that it is common in human mission designs for the aeroshell to be integral with vehicle's primary structure. Study has shown that such a configuration results in a net increase in the payload delivered to the Martian surface.<sup>8</sup> Therefore, the backshell used for Mars entry is not discarded in this study.

*Heatshield.* Heatshield sizing was split into two distinct segments: the first involves calculating the amount of ablative TPS material required for protection during Mars aerocapture and entry, while the second estimates the mass of the underlying structure. The TPS mass was estimated by calculating the required thickness at the stagnation point of the heatshield (this thickness was computed using 1-D finite difference heat transfer calculations)<sup>7</sup> For this analysis, the ablative material PICA (phenolic impregnated carbon ablators, recently used on the Stardust mission<sup>9</sup>) was assumed for the TPS material. It was also assumed that the heat rate observed by the heatshield decreased as a cosine function with distance from the stagnation point. Recognizing that PICA has a density of 227 kg/m<sup>3</sup>, the TPS mass can be calculated. Note that in the dual-use heatshield scenario, where the same heatshield is used for Mars aerocapture and entry, the total required thickness at the stagnation point was estimated as the sum of the required thickness for each individual stage. The underlying heatshield structure was estimated as 10% of the total entry mass.

*Propulsion.* The primary propulsion system consists of a liquid bipropellant engine using methane (CH<sub>4</sub>, density of 422.6 kg/m<sup>3</sup>) and liquid oxygen (LOX, density of 1140.1 kg/m<sup>3</sup>).<sup>10</sup> This propellant choice was made to remain consistent with most previous human Mars exploration studies<sup>8,11,12</sup> as well as NASA's Exploration Systems Architecture Study (ESAS).<sup>13</sup> Use of a LOX/CH<sub>4</sub> propulsion system for descent is also desirable to maximize commonality with the ascent stage and other chemical propulsion devices (which are slated to use in-situ resource utilization and produce methane from CO<sub>2</sub> in the Martian atmosphere). Furthermore, a LOX/CH<sub>4</sub> system can obtain a specific impulse on the order of 350 seconds at a mixture ratio of 3.5.<sup>14,15</sup> For the purposes of

propellant tank sizing, it was assumed that the operating pressure was approximately 1.38 MPa (burst pressure  $\sim 2.76$  MPa) with a tank factor<sup>10</sup> of 6,250 m (corresponding to a titanium tank). The total mass of propellant was calculated by integrating the equations of motion during powered descent.

*Reaction Control System.* The vehicle's RCS configuration was largely based on the Apollo command module design as well as the current CEV design proposed in the ESAS final report.<sup>13</sup> The RCS is equipped with 12 thrusters similar to ones used on Apollo. Each thruster weighs 3.8 kg and uses the reliable propellant combination of monomethyl hydrazine (MMH, density of  $878 \text{ kg/m}^3$ )<sup>10</sup> and nitrogen tetroxide ( $\text{N}_2\text{O}_4$ , density of  $1440 \text{ kg/m}^3$ ).<sup>10</sup> The thrusters operate at a mixture ratio of 2.16, yielding a specific impulse of approximately 289 seconds. The propellant tanks were sized in a fashion similar to that of the main propulsion system.

*Overview of Sizing Results.* Analysis of the mass sizing results begins by comparing scenarios that propulsively decelerate from Mach 3 without the use of parachutes. Parachutes are not included in this initial assessment due to the large uncertainty in their mass. By looking at propulsive options only, this initial comparison may be used to identify the most promising heatshield strategy (dual-use vs. single-use) and lift-to-drag ratio. The results of this analysis, summarized in Figure 10, show the percentage of total mass consumed by the EDL system as a function of mass at entry.

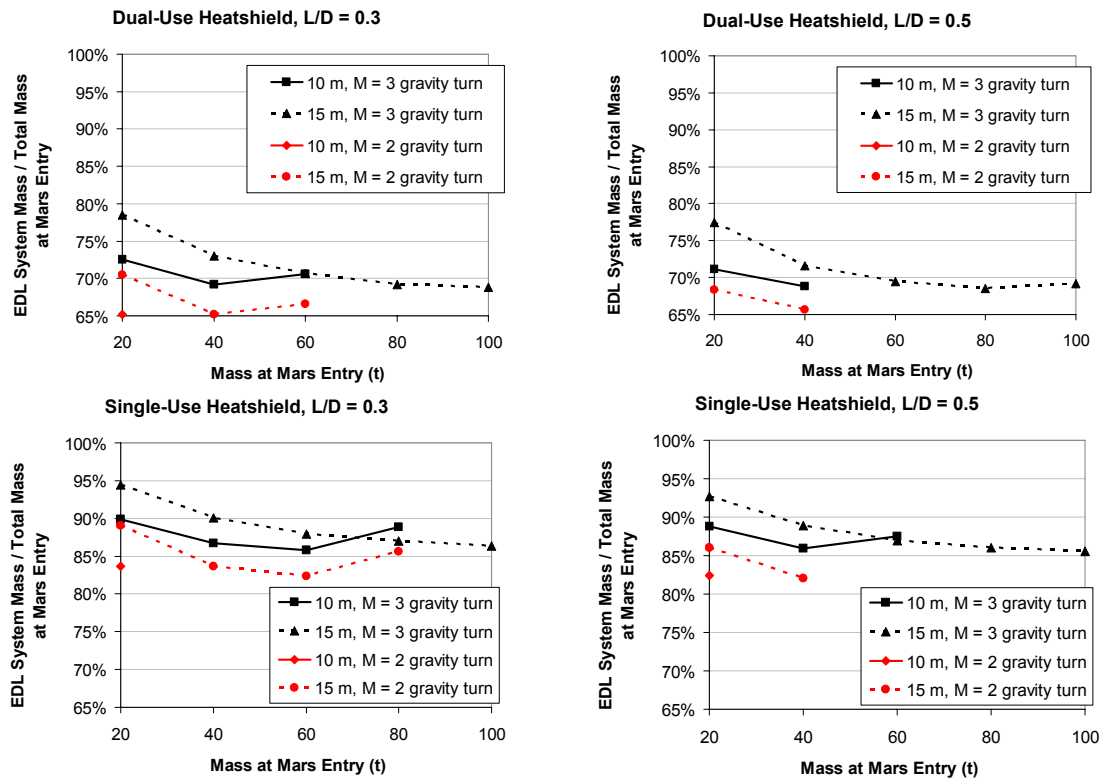


**Figure 10** Percentage of total mass at entry consumed by EDL related systems. Percentages are representative of cases where the Mars aerocapture velocity is 6 km/s.

These trends are depicted for both single-use and dual-use heatshields under various lift-to-drag ratios. Furthermore, each curve in this figure is truncated when the vehicle impacts the ground before engine ignition if it can no longer land without exceeding the maximum allowable g-limit. The cases illustrated in Figure 10 correspond to those with an initial velocity at Mars aerocapture of 6 km/s (note that similar trends and magnitudes were observed for cases with a velocity of 8.8 km/s).

The lightest EDL system employs a dual-use heatshield, has a L/D of 0.3, and initiates the gravity turn at Mach 2. However, this EDL architecture is limited to entry masses below 60 t (see Figure 9). For this case, an EDL mass fraction on the order of 0.5 is required, limiting the human exploration payload to a maximum of 30 t. Given the expected scope of human Mars missions, this payload mass allocation may be deemed unacceptable. For larger entry masses, the gravity turn must be initiated at Mach 3.

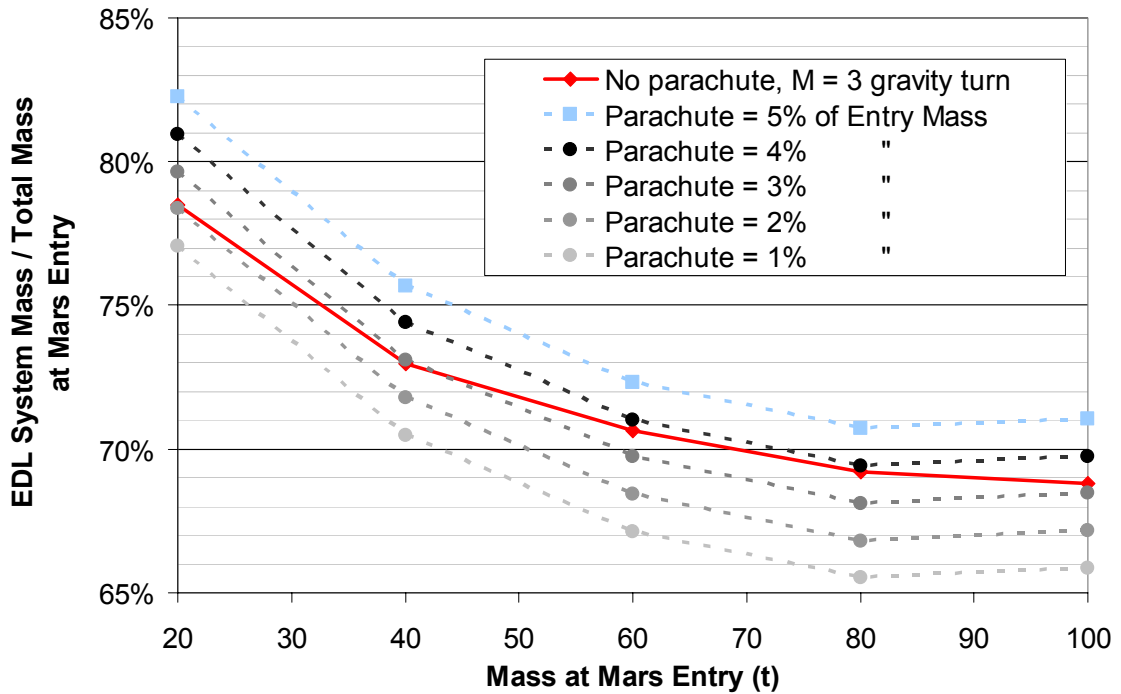


**Figure 11 Percentage of total mass at entry consumed by EDL related systems for various mass fractions. This data corresponds to a vehicle diameter of 15 m and 0.3 L/D.**

Using this scenario as a point of departure, the potential advantages of a parachute system were assessed (see Figure 11). Note that the mass fractions shown in this figure correspond to descent trajectories where the parachute diameter is not permitted to exceed 30 m. Examination of these results shows that the parachute-augmented system is superior as long as the parachute mass does not exceed 2% - 4% of the Mars entry mass and is deployed at Mach 3.

A mass-based comparison was performed between the best propulsive-only option and the corresponding parachute case. If the parachute system is assumed to

account for 3% of the entry mass, Figure 11 indicates that the parachute option should outperform the propulsive-only option for systems in excess of 40 t. Assuming an entry mass of 60 t, a comparison of the mass breakdowns for both scenarios is illustrated in Figure 12. In this example, the system equipped with a parachute is capable delivering a payload mass fraction of 0.33 to the surface, while the propulsive-only option can only deliver a payload mass fraction of 0.29.

Given the fidelity of this mass sizing analysis, these two payload mass fractions are deemed essentially the same and the likelihood of a parachute system to provide terminal descent deceleration for a human exploration mission is considered low.

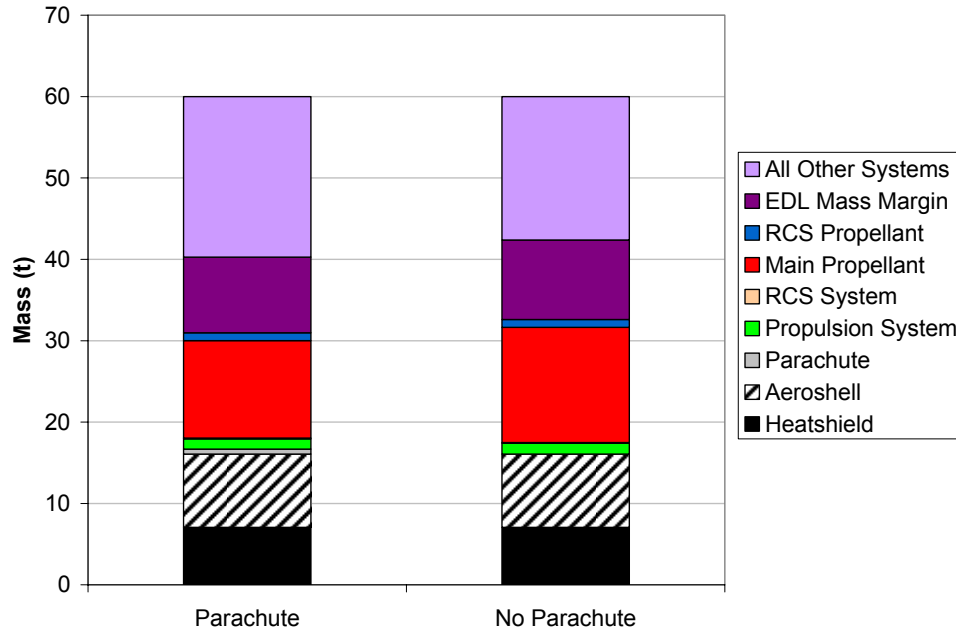


**Figure 12 Mass breakdowns for 15 m diameter, 60 t, dual-use heatshield vehicle with and without a parachute, 0.3 L/D.**

## CONCLUSION

This investigation presented a potential entry, descent and landing sequence for Mars human exploration architecture derived from an extension to current robotic approaches. An aerocapture corridor width analysis suggests that a L/D of 0.3 is sufficient for Mars aerocapture across a large velocity range (6 - 8.8 km/s). Analysis of the entry phase shows that large mass systems (greater than ~50 t - 60 t) cannot reach Mach 2 except at potential landing sites in the northern hemisphere of Mars. This suggests that large mass payloads may have to be broken down into smaller pieces and brought together on the surface if more scientifically interesting sites at higher elevations are to be explored.

Analysis of propulsive descent shows thrust and  $\Delta V$  requirements which are reasonably achieved but whose mass requirements significantly limit the amount of landed mass for a given vehicle entry mass. From a propulsion standpoint, it is desirable

to initiate the terminal descent burn at a low Mach number which does not lie on the divergent portion of the thrust curves shown earlier. Such a choice for burn initiation Mach number can minimize the sum of required propellant mass and engine mass. Parachutes can partially ease propulsion requirements by permitting large mass vehicles to aerodynamically decelerate to lower velocities before burn initiation, leading to significant decreases in the thrust requirement. Even with parachutes,  $\Delta V$  requirements remain on the order of 700 m/s in the best of the cases examined, implying that on the order of at least 20% of a vehicle's entry mass must be propellant.

Because of expected landed mass requirements, it is concluded that Mars human exploration aerocapture and EDL systems will have little in common with current and next-decade robotic systems. As such, significant technology and engineering investment will be required to achieve the EDL capabilities required for a human mission to Mars. Technology advances that require further analysis include aerocapture, ISRU, high Mach aerodynamic deceleration concepts other than parachutes, supersonic propulsive descent capabilities, and thermal protection and structural concepts for large diameter aeroshell systems.

## REFERENCES

1. Z.R. Putnam, et al. "Entry System Options for Human Return from the Moon and Mars," AIAA 2005-5915, *AIAA Atmospheric Flight Mechanics Conference*, San Francisco, CA, August 2005.
2. W.K. Hofstetter, P.D. Wooster, W.D. Nadir, E.F. Crawley, "Affordable Human Moon and Mars Exploration through Hardware Commonality," AIAA Paper 2005-6757, *Space 2005*, Long Beach, California, 30 Aug - 1 Sep 2005.
3. K.T. Edquist, "Afterbody Heating Predictions for a Mars Science Laboratory Entry Vehicle," AIAA Paper 2005-4817; *38th AIAA Thermophysics Conference*, Toronto, Ontario, Canada, 6-9 Jun. 2005 .
4. A.A. Wolf, C. Graves, R. Powell, W. Johnson, "Systems for Pinpoint Landing at Mars", *Advances in the Astronautical Sciences*, Volume 119, 2677-2696 , 20050101; 2005.
5. B.K. Muirhead, F. Naderi, M. Sander, J. Simmonds, M. Meyer, J. Baker, C. Whetsel, G. Udomkesmalee, A. Green, "Mars Science Laboratory - Mission Concept Review", Jet Propulsion Laboratory, National Aeronautics and Space Administration, Pasadena, CA October 28, 2003.
6. T.C. Duxbury, R.L. Kirk, B.A. Archinal, G.A. Neumann, "Mars Geodesy/Cartography Working Group Recommendations on Mars Cartographic Constants and Coordinate Systems," *Symposium on Geospatial Theory, Processing and Applications*, Ottawa, 2002.
7. J.A. Dec, R.D. Braun, "An Approximate Ablative Thermal Protection System Sizing Tool for Entry System Design," *AIAA Aerospace Sciences Conference*, Reno, NV, January 2006.
8. B.G. Drake, "Reference Mission Version 3.0, Addendum to the Human Exploration of Mars: The Reference Mission of the NASA Mars Exploration Study Team," NASA Johnson Space Center, EX13-98-036, June 1998.

9. H.K. Tran, C.E. Johnson, D.J. Rasky, F.C.L. Hui, M. Hsu, Y.K.Chen, "Phenolic Impregnated Carbon Ablators (PICA) for Discovery Class Missions," AIAA Paper 1996-1911, *31<sup>st</sup> Thermophysics Conference*, New Orleans, Louisiana, 17-20 June 1996.
10. R.W. Humble, G.N. Henry, W.J. Larson, "Space Propulsion Analysis and Design," McGraw-Hill Companies, Inc. 1995.
11. B. Griffin, B. Thomas, D. Vaughan, B. Drake, L. Johnson, G. Woodcock, "A Comparison of Transportation Systems for Human Mission to Mars," AIAA Paper 2004-3834, *40<sup>th</sup> AIAA/ASME/SAE/ASEE Joint Propulsion Conference and Exhibit*, Fort Lauderdale, Florida, 11-14 July 2004.
12. R.M. Zubrin, D.A. Baker, O. Gwynne, "Mars Direct: A Simple, Robust, and Cost Effective Architecture for the Space Exploration Initiative," *29th AIAA Aerospace Sciences Meeting*, Reno, Nevada, 7-10 January 1991.
13. "NASA's Exploration Systems Architecture Study: Final Report," National Aeronautics and Space Administration, NASA-TM-2005-214062, November 2005.
14. J. Hopkins, "Comparison of Propulsion Options for a Lunar Lander Ascent Stage," AIAA Paper 2005-6740, *AIAA Space 2005*, Long Beach, California, 30 August – 1 September 2005.
15. D. Preklik, G. Hagemann, O. Knab, L. Brummer, C. Mading, D. Wiedmann, P. Vuillermoz, "LOX/Hydrocarbon Propellant Trade Considerations for Future Reusable Liquid Booster Engines," AIAA Paper 2005-3567, *41<sup>st</sup> AIAA/ASME/SAE/ASEE Joint Propulsion Conference and Exhibit*, Tucson, Arizona, 11-13 July 2005.